Acoustic Doppler and Angle of Arrival Wind Detection and Comparisons with Direct Measurements at a 300 m Mast

G. PETERS, C. WAMSER AND H. HINZPETER

Meteorological Institute, University of Hamburg, Hamburg, West Germany

(Manuscript received 8 August 1977, in final form 7 April 1978)

ABSTRACT

Wind measurements estimated using acoustic sounding systems are compared with direct measurements obtained at a 300 m antenna mast. Different meteorological periods, including very stable to unstable stratification and weak to strong winds, were investigated. It is demonstrated that satisfactory results may be obtained using a simple monostatic Doppler device combined with an appropriate evaluation method. Preliminary tests on an angle of arrival sodar system showed its ability to obtain reasonable wind measurements at least under stable conditions.

1. Introduction

Investigations during the past 10 years have shown that quantitative measurements of wind velocity by acoustic sounding techniques are possible. The emphasis of previous developments concerned the utilization of the received signal Doppler shifts. Several sophisticated systems have been demonstrated to be effective for remote measurements of wind profiles in the lower atmosphere (e.g., Beran *et al.*, 1971; Beran and Clifford, 1972; Aubry, 1975; Hall *et al.*, 1975; Owens, 1977). On the other hand, much less experience has been accumulated using the angle of arrival (AOA) method. To our knowledge McAllister (1972) and Mahoney *et al.* (1973) have been the only ones to report to date on the feasibility of this method.

A basic requirement for the development of remote sensing systems is the verification of the data by direct measurements. Comparisons with mast or balloonborne sensor package data have been presented, for example, by Beran and Willmarth (1971), Balser *et al.* (1976) and Gaynor (1977).

In this paper the applicability of the above wind measuring methods for studies in situations with very different thermal stratification and wind velocity conditions is described. A unique advantage of these investigations was the availability of a fully equipped 300 m antenna mast at the measuring site. This facilitated direct determination of the wind, temperature and turbulence field by sensitive *in situ* sensors.

A relatively simple Doppler and an AOA sodar system were in operation at the site between January and May 1977. The intent of these investigations was to establish the extent of agreement between direct and acoustic wind measurements and to identify and account for any observed systematic differences.

Section 2 summarizes principles and some theoretical aspects of Doppler and AOA techniques. In Sections 3 and 4 the site and instrumentation are described and results for the different meteorological conditions are presented. The case studies include a short discussion of errors introduced by a straightforward signal averaging procedure (center of gravity) and the improvement which may be realized by a more adequate signal evaluation based on the frequency distribution of the signal (peak frequency).

2. Theoretical aspects of Doppler and AOA techniques

a. Doppler

Sound propagation in the atmosphere is determined by inhomogeneities of temperature, wind, and to a lesser extent by constituents like water vapor. According to the scale of the inhomogeneity the interaction of sound with the atmosphere may be conveniently divided into scattering and refraction. Small-scale inhomogeneities on the order of the acoustic wavelength cause scattering of sound and are the basis for active acoustic sounding. Particular details of the sound scattering and generation of Doppler shifts need not be presented here as many adequate references exist (e.g. Monin, 1962; Ottersten, 1969; Tatarskii, 1971; Brown, 1972, 1974).

Doppler measurements can be carried out in either a single antenna monostatic configuration or a variety of separated antenna bistatic configurations. The greater complexity of the equipment in bistatic systems is counterbalanced by a better signal-to-noise ratio. Whereas the monostatic signal intensity depends only on temperature fluctuations, in the bistatic mode

0021-8952/78/1171-1178$05.00

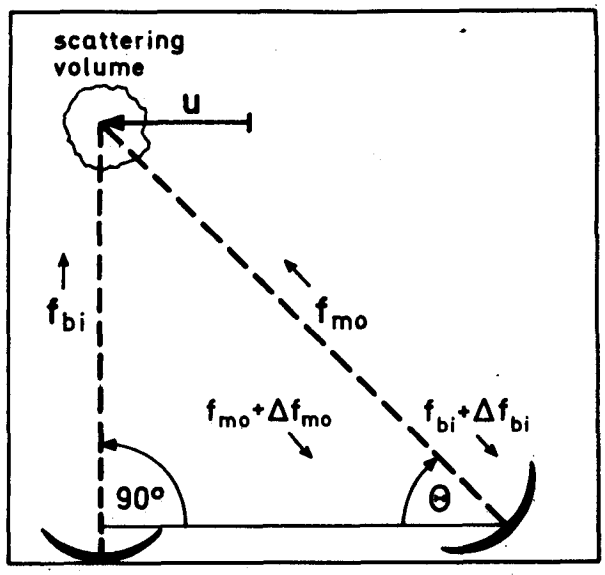

FIG. 1. Geometry for monostatic and bistatic Doppler wind sensing.

velocity fluctuations also contribute to the scatter intensity.

Our Doppler measurements are based on both configurations. In the monostatic mode the azimuth of the tilted antenna (SODAR I) was adjusted to the direction of the mean surface wind. In the bistatic mode an additional vertically pointed antenna (SODAR II) at a distance of 120 m was used as transmitter. The corresponding scattering geometry is shown in Fig. 1. The Doppler shift Δf_{bi} is proportional to the wind component parallel to the bisector of the antenna beams. Δf_{mo} is proportional to the radial wind component. The basic Doppler shift equation reads

$$\Delta f = (1/2\pi)(\mathbf{K}_s - \mathbf{K}_0)\cdot\mathbf{u}, \tag{1}$$

where $\mathbf{K}_0$, $\mathbf{K}_s$ are the vectors of the wavenumbers of the transmitted and the scattered sound. Assuming the mean wind u to be horizontal, $|\mathbf{K}_s| \approx |\mathbf{K}_0|$, and $\mathbf{K}_0$ to be vertical the relation between the Doppler shift and u is given by

$$\Delta f_{bi} = -(u f_{bi}/c)\cos\theta \tag{2}$$

and in the monostatic case ($\mathbf{K}_s = -\mathbf{K}_0$) by

$$\Delta f_{mo} = -(2u f_{mo}/c)\cos\theta, \tag{3}$$

where c is the speed of sound, f the transmitted frequency and θ the antenna elevation.

There are a number of papers which consider the validity of these relationships. Systematic errors are produced by atmospheric sound refraction. From the analysis by Beran and Clifford (1972) and by Spizzichino (1974), we conclude that in our antenna configuration this error is smaller than 0.5 m s^{-1}. More serious are random variations of the measured Doppler shift which, according to our experience, are typically in the order of ±10 Hz for an operating frequency of 1680 Hz. Different mechanisms contributing to this effect have been considered by several authors. Ford and Meecham (1960) calculated the spectral broadening which is produced by turbulent motion within the scattering volume. Brown and Clifford (1973) gave an expression for the spectrum of an acoustic pulse traveling through a turbulent medium with transverse wind. Brown (1974) considered the combined effects of a finite beamwidth and transverse wind for the case of backscatter. The Doppler variations predicted by these studies are small compared with the observed variations. A significant contribution, however, can be produced by an inhomogeneous reflectivity distribution within the scattering volume (Spizzichino, 1974). The resulting standard deviation of the Doppler wind fluctuations is of the order of

$$\sigma_u = u(\beta/2)\tan\theta, \tag{4}$$

where β is the beamwidth. A typical value for σ_u is about ±1 m s^{-1}, for $u = 5$ m s^{-1}, $\theta = 65°$ and $\beta = 10°$ which is the beamwidth of the SODAR I antenna.

b. Angle of arrival

The influence of the wind and temperature profiles on sound propagation can be calculated by means of geometric optics. Thompson (1974) derived the following ray equations for a stratified moving medium from the hydrodynamic equations:

$$\frac{\partial x}{\partial z} = \pm\frac{uB + c^2c_0^{-1}\sin\varphi_1}{c(B^2 - c^2c_0^{-2}\sin^2\varphi_1 - c^2c_0^{-2}\sin^2\varphi_2)^{\frac{1}{2}}}, \tag{5}$$

$$\frac{\partial y}{\partial z} = \pm\frac{vB + c^2c_0^{-1}\sin\varphi_2}{c(B^2 - c^2c_0^{-2}\sin^2\varphi_1 - c^2c_0^{-2}\sin^2\varphi_2)^{\frac{1}{2}}}, \tag{6}$$

where

$$B = 1 - (u/c_0)\sin\varphi_1 - (v/c_0)\sin\varphi_2,$$

u, v are the horizontal wind components, φ_1, φ_2 the initial components of the inclination of the wave front normal and c_0 is the initial sound speed. The signs correspond to up- and down-running rays. If $\varphi_{1,2}$ and $u/c, v/c \ll 1$, and we neglect terms of higher order in $\varphi_{1,2}$ and $u/c, v/c$, the equations become

$$\left\{\frac{\partial x}{\partial z}, \frac{\partial y}{\partial z}\right\} = \pm\left\{\frac{u}{c} + \frac{c}{c_0}\varphi_1, \frac{v}{c} + \frac{c}{c_0}\varphi_2\right\}. \tag{7}$$

If we consider a height range of some hundred meters and exclude cases with $\varphi_{1,2} \gg u/c, v/c$, only a small error is introduced by assuming $c = c_0$, i.e.,

$$\left\{\frac{\partial x}{\partial z}, \frac{\partial y}{\partial z}\right\} = \pm c_0^{-1}\{u + c_0\varphi_1, v + c_0\varphi_2\}. \tag{8}$$

For a monostatic sounder the total displacement, i.e., the integral of the ray equations from the antenna

TABLE 1. Instrumentation at the site.

System	Height (m)	Measured quantities	Symbol key	Instruments
Mast	250	w', T', U, D, $\bar{T}$	w' fluctuations of the vertical wind component	Sonic anemometer
	175	w', U, $\bar{T}$		
	110	w', T', U, D, $\bar{T}$	T' temperature fluctuations	Sonic thermometer
	70	$\bar{T}$	U horizontal wind velocity	Cup anemometer
	50	w', T' U, D, $\bar{T}$	D wind direction	Wind vane
	10	U, D, $\bar{T}$, $\bar{T}_f$	$\bar{T}$ mean temperature	PT-100
	2	w', T' $\bar{T}$	$\bar{T}_f$ wet-bulb temperature	PT-100
Sonde	0–280	T_s, T_s', D_s, U_s, w_s'		U_s, w_s'—Gill propeller
SODAR I	Doppler	280 m NE of the mast		$\bar{T}_s$, T_s'—thermistors
SODAR II	AOA	210 m ENE of the mast		D_s—potentiometer

to the scattering volume and return, must be zero. For a vertically pointing sounder this condition leads to

$$\{\varphi_1,\varphi_2\} = -2c^{-1}\{\bar{u},\bar{v}\} \tag{9}$$

for the backscattered ray, where

$$\{\bar{u},\bar{v}\} = h^{-1}\int_0^h \{u,v\}dz.$$

Thompson's equations describe two effects: first, the transport of the sound energy by the wind and, second, the change of the wave front direction due to refraction. The simplified Eq. (8) obviously represents a case where the second effect can be neglected. The direction of this ray is given at any point by the superposition of the wind vector and the initial sound velocity vector relative to the medium.

As the initial wave front direction $\varphi_{1,2}$ of the ray is retained until it reaches the sounder it can be measured there. It is determined in our case by the apparent velocity components

$$\{t_1,t_2\} = \left\{u_R+\frac{c}{\varphi_1}, v_R+\frac{c}{\varphi_2}\right\}, \tag{10}$$

where u_R, v_R are the wind velocity components at the receiver level. As u_R, $v_R \ll c/\varphi_{1,2}$ this may be neglected. The apparent velocity is obtained from the phase difference ϕ at receiver points spaced by d:

$$\{t_1,t_2\} = 2\pi f\left\{\frac{d_1}{\phi_1},\frac{d_2}{\phi_2}\right\}. \tag{11}$$

Eqs. (9), (10) and (11) give the final relation for the phase difference and the mean wind between sounder and scattering volume:

$$\{\phi_1,\phi_2\} = (4\pi f/c^2)\{d_1\bar{u},d_2\bar{v}\}. \tag{12}$$

If there are more levels of sufficient scatter intensity, wind profiles can be obtained by the relation

$$(1/\Delta h)[\{\phi_1(h),\phi_2(h)\}h-\{\phi_1(h+\Delta h),\phi_2(h+\Delta h)\} \times(h+\Delta h)] = (4\pi f/c^2)\{d_1\bar{u},d_2\bar{v}\}, \tag{13}$$

where

$$\{\bar{u},\bar{v}\} = (1/\Delta h)\int_h^{h+\Delta h}\{u,v\}dz.$$

A detailed discussion of the operating conditions and some consideration of possible principle error sources of the AOA technique can be found in Peters (1977).

3. Site, instrumentation and data handling

The experiments were performed at a site which is situated at the southeast border of the urban area of Hamburg in the flat marshland of the river Elbe. The direct measurements were carried out at a 300 m tubular antenna mast (diameter 2 m). The sensors for wind, temperature and turbulence are located on several 5 m long booms which are directed to the south-southwest. In addition to the fixed-level sensors, a motor driven pulley system was installed for operating a sensor package up to a height of 280 m. Tower instrumentation, the tethered sonde and location of the SODAR systems are summarized in Table 1. For a detailed description of the facility see Wamser and Müller (1977) and Stilke *et al.* (1976).

The antenna of SODAR I is a horn paraboloid with an aperture of 1.2 m. By means of a motor driven steerable pedestal both azimuth and elevation may be adjusted. In addition to a linear amplitude detector an FM discriminator is implemented to obtain

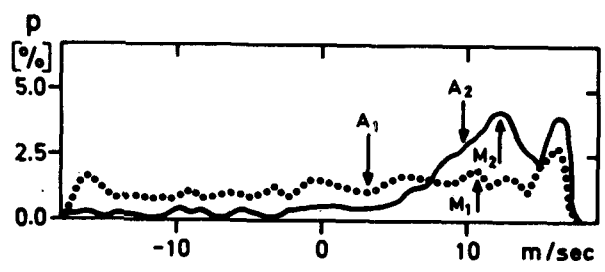

FIG. 2. Doppler frequency distributions measured with the phase-lock loop (PLL). Solid line, high S/N; dotted line, low S/N. The arrows indicate center of gravity (A) and peak frequencies (M).

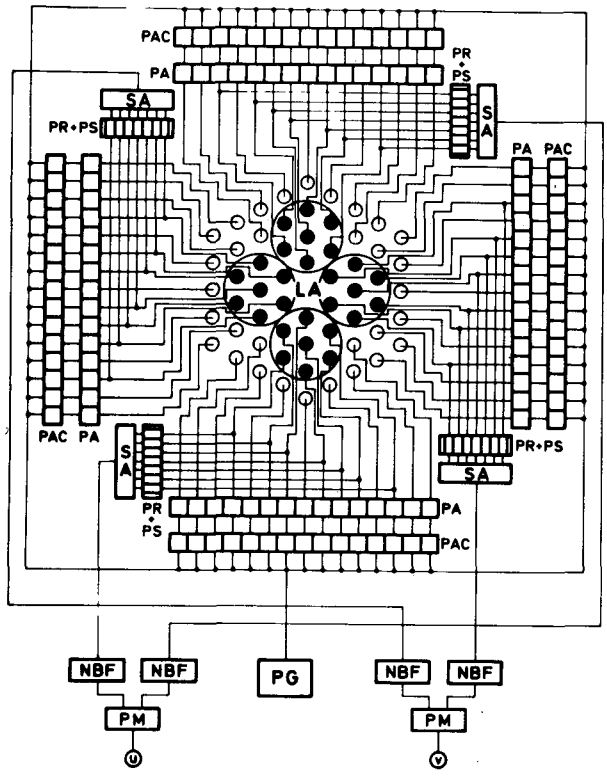

FIG. 3. Schematic of the phased array and its electronics. The grouped full circles (subarrays) form a pair of orthogonal interferometers.

the Doppler shift in a maximum range of ±45 Hz. The FM discriminator consists of a phase-lock loop (IC TYPE SE 565) with a special wiring for small frequency deviations. The cutoff frequency of the PLL low-pass filter is 300 Hz. Normally a transmitting frequency of 1685 Hz and a pulse length of 0.1 s have been used. The 3 dB beam width was about 10°.

The evaluation of the phase-lock loop-output signal requires care. This becomes apparent by inspection of the signal distributions. Two typical examples for high and low signal-to-noise ratio (S/N) are presented in Fig. 2. Even for high S/N the width of the distribution is considerable. This may be due to turbulent spectral broadening as well as to the specific behavior of the PLL. The peaks at the limits of the measuring range are produced artificially by the nonlinear behavior of the PLL at these points. These distortions are the reason for a systematic underestimation of the wind by averaging of the PLL signal (center of gravity, COG). On the other hand, it may be assumed that the maximum within the linear range (M_1,M_2) is a better measure for the mean wind.

The AOA–SODAR was designed and constructed by Peters (1977). The characteristic feature of this system is an array of 61 horn loudspeakers which are tuned with respect to phase in both the transmitting

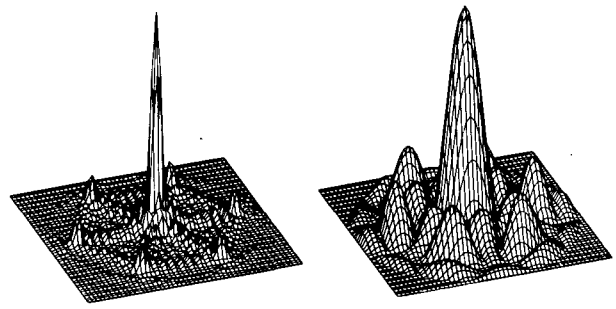

FIG. 4. Computed antenna beam patterns of SODAR II, linear amplitude (no enclosure). Left, whole array; right, one subarray.

and receiving mode. Fig. 3 is a block diagram of the phased array and its associated electronics. The angle of arrival is obtained by the phase differences of selected pairs of subarrays, each forming an interferometer. Different interferometer configurations have been applied, only one example is indicated by the grouped full circles.

The performance and capability of the AOA method is dependent on the narrowness of the transmitted lobe to even a higher degree than the Doppler method. It is for this reason that such a great number of loudspeakers has been used, giving a 3 dB beamwidth of about 6°. Computed beam patterns of the whole array and of one receiving subarray (Fig. 4) have been compared with measured patterns by a balloonborne microphone, one example of which is shown in Fig. 5. Some improvement in these patterns is to be expected by the 2.5 m cylindrical enclosure used for the AOA measurements.

The phase differences have been measured by conventional analogue phase meters with a range of $\pm\pi$. As this range is frequently exceeded by random

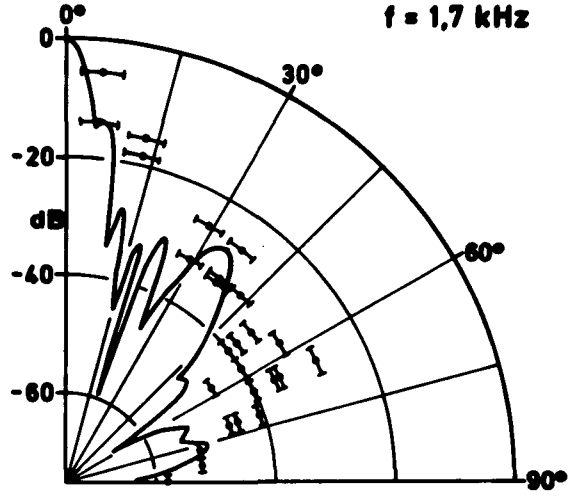

FIG. 5. Comparison between computed (solid lines) and measured (points) antenna gain function (no enclosure).

TABLE 2. Summary of the investigated cases. COG: center of gravity method (averaging). PF: peak frequency method.

1977 date	Time interval (LT)	Meteorological situation	Doppler monostatic	Doppler bistatic	Angle of arrival	Direct measurement
13 January	1530–2030	near neutral to slightly stable; $3 \leqslant U_{175} \leqslant 10$ [m s^{-1}]	no	COG	no	yes
10, 11 May	1200, 1030	day: neutral/convective, night: stable; $2 \leqslant U_{175} \leqslant 14$ [m s^{-1}]	COG	no	no	yes
19 May	0330–0630	ground based inversion $h_{inv} \approx 250$ m $11 \leqslant U_{175} \leqslant 16$ [m s^{-1}]	COG/PF	no	PF	yes
12 March	1530–2000	free inversion (~180–200 m) $1 \leqslant U_{175} \leqslant 5$[m s^{-1}]	no	no	PF	yes

fluctuations, distortions of the signal distribution occur. Therefore, similar to the PLL Doppler signal, the center of gravity underestimates the AOA wind. For this reason, the unreduced sodar data were digitized with a sampling rate of 200 Hz and the maxima of the frequency distributions of the Doppler and the AOA for different range gates determined.

4. Results and discussion

In the following, results of four different meteorological cases are shown. Table 2 summarizes the stability and wind conditions and the remote sensing methods in operation.

a. Doppler, center of gravity (COG) method

In order to demonstrate the degree of wind underestimation by averaging of the PLL output signal, two examples both for bistatic and monostatic configurations and different meteorological conditions have been analyzed. In the bistatic mode the receiving antenna was tilted 35°, so that significant signal could be obtained from the height range 120–250 m with maximum sensitivity at 175 m (height of an instrumented tower platform). From the direct wind measurements at 175 m the component parallel to bistatic Doppler basis was determined. The result is to be seen in Fig. 6. Although the general slopes of the directly and indirectly measured wind values agree quite well, the Doppler wind is systematically too low.

Fig. 7 shows a comparison for the monostatic mode during a 24 h period. Again the Doppler wind follows the general trend of the actual wind quite well but with considerable underestimation. This underestimation has also been observed for all other cases to which this evaluation method was applied. Unfortunately the correlation between direct and Doppler wind is not strong enough for an effective subsequent correction.

b. Doppler, peak frequency (PF) method

On 19 May 1977 the wind was measured both by the Doppler shift and the AOA methods. In addition to the COG method, the Doppler wind was derived by determining the maximum of the frequency distribution of the PLL output. The comparisons with the direct measurements at three different heights are presented in Fig. 8 which shows an excellent agreement.

In spite of the extremely high backscatter intensities from all levels during this period the COG method again significantly underestimated the wind.

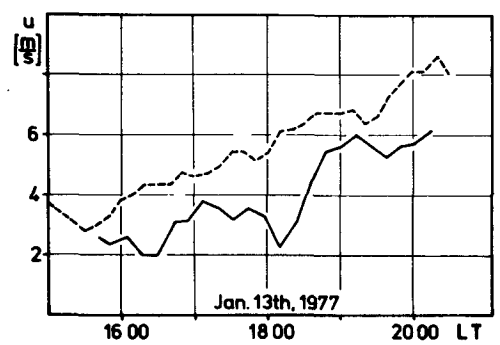

FIG. 6. Comparison between bistatic Doppler and directly measured wind. u_{Dopp}: solid line (175 m); u_{dir}: dashed line (175 m).

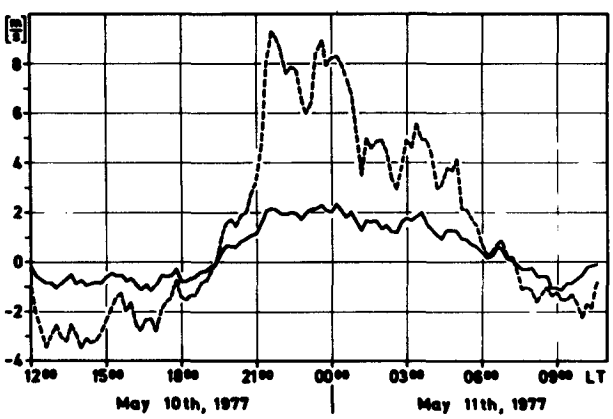

FIG. 7. Comparison between monostatic Doppler (averaging method) and directly measured wind. u_{Dopp}: solid line (70 m); u_{dir}: dashed line (50 m).

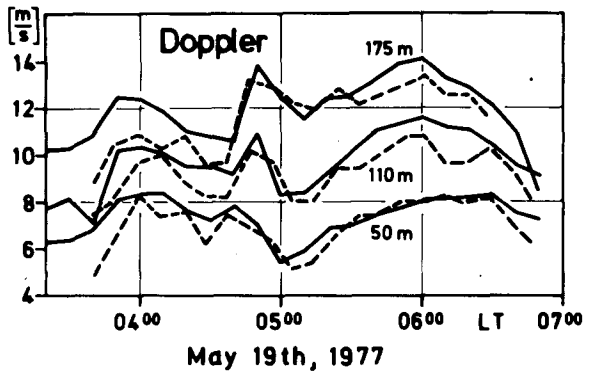

FIG. 8. Comparison between Doppler (peak-frequency method) and directly measured wind. u_{Dopp}: dashed line; u_{dir}: solid line.

A summary of the performance of the different evaluation methods is given in Fig. 9. The solid regression lines (crosses, circles, points) refer to the COG method for the different cases and exhibit very different slopes. The broken regression line through the triangles with a slope of nearly 45° and a correlation coefficient of 0.94 reveals the improvement which is achieved by the PF method.

c. Angle of arrival

The performance of the AOA method is demonstrated for two meteorological situations. One case is characterized by overcast sky and by rather weak winds up to several hundred meters with wind directions turning gradually from southwest to north. At 1720 LT a free inversion developed at a height of

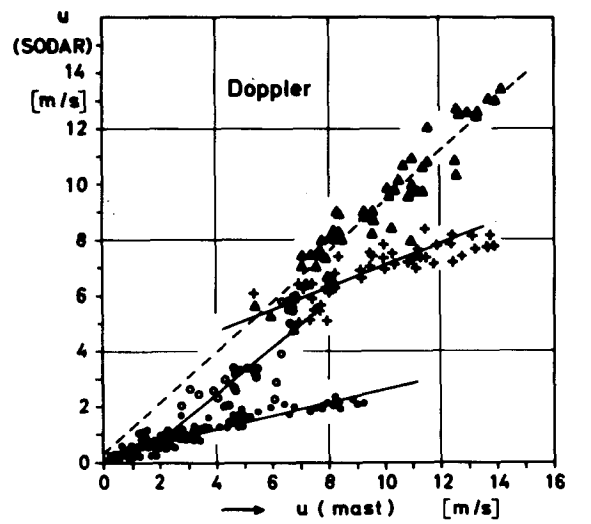

FIG. 9. Regression for different cases and evaluation methods. Every symbol refers to a 10 min sampling period.

Points	10 May 1977, COG
Circles	13 Jan. 1977, COG
Crosses	19 May 1977, COG
Triangles	19 May 1977, PF

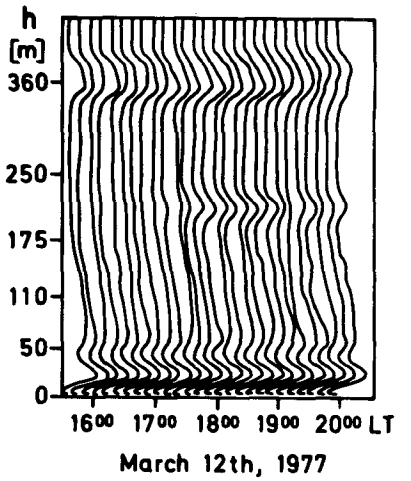

FIG. 10. SODAR II mean profiles of the relative backscatter amplitude.

~200 m which clearly can be seen by the backscatter maxima in Fig. 10.

The broader maxima at 360 m are caused by re-

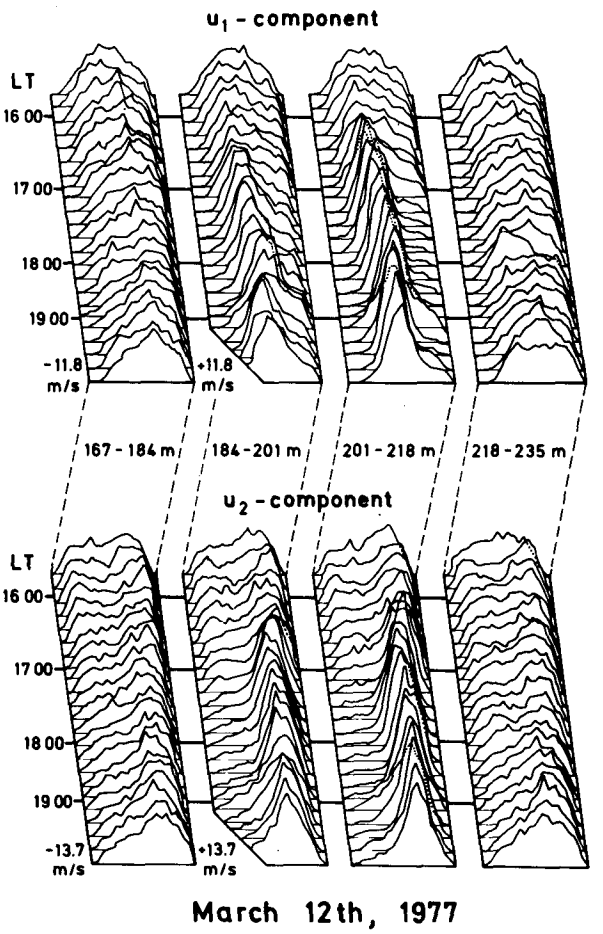

FIG. 11. Frequency distributions of the phase differences of the arriving backscatter signal for two orthogonal directions and four height ranges.

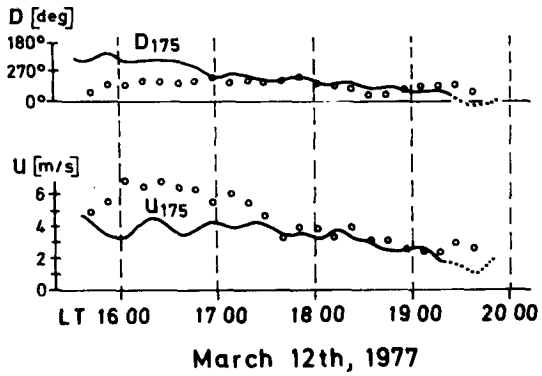

FIG. 12. Mean wind direction and velocity between surface and 175 m. Points: AOA; solid line; direct (dotted part, disturbed by the mast).

flection of the antenna mast. Frequency distributions of the phase differences ϕ_1, ϕ_2 for four different levels are shown in Fig. 11.

The mean wind between the surface and the inversion was determined by the position of the peak frequencies. The results are summarized in Fig. 12. Good agreement between the direct and AOA wind values is only achieved from the inversion layer. It corresponds to the significant narrow maxima after about 1720 LT in Fig. 11 for the two height ranges 184–201 and 201–218 m. For all levels below the inversion the distributions show less defined peaks even when the S/N was higher than within the inversion. Attempts to derive the wind from these levels were not successful. This failure has also been observed for other cases with convective conditions. A satisfying interpretation for this cannot be given at the present time although we feel that different stability dependent mechanisms, such as phase front distortions close to the transmitter and receiver (Brown and Clifford, 1977) and the reflectivity distribution within the scattering volume, contribute to this failure. It is expected that a more adequate signal processing of the AOA based on the determination of the phase spectrum will lead to an essential improvement.

The other case for which AOA measurements are presented is 19 May 1977. This is a period with very strong easterly winds up to about 20 m s^{-1} at 250 m and extraordinarily great wind shear above the inversion. Due to the cloudless sky during the night, an inversion up to at least 250 m was formed. The variation of the inversion height is reflected clearly by the backscatter profiles of Fig. 13. Usable AOA information was obtained from the whole range of the inversion, so Eq. (12) could be applied to derive wind profiles.

In Fig. 14 the AOA wind is presented for two height ranges and shows good agreement with the directly measured wind velocities. For these two stable cases the regression line has a slope of about 45° with a correlation coefficient of 0.97.

5. Concluding remarks

One reason for the worldwide interest and application of atmospheric echo sounding has been its relatively low cost. Quantitative wind measurements, however, have been performed in recent years only with increasingly complex equipment and sophisticated evaluation techniques and thus much of the original cost effectiveness has been lost. In this paper we have demonstrated that by using monostatic systems and by relatively simple evaluation methods the determination of reliable mean wind values up to about 200 m is possible. The peak frequency method, however, requires sampling intervals of some minutes' duration in order to achieve sufficient statistical stability. If sodar is to be used for the investigation of short-time variations of the wind field more sophisticated signal processing methods such as Fourier analysis are necessary.

Continuous Doppler and AOA wind profiles have been measured but only values from those levels at which direct wind measurements were available have been presented here. The inspection of the profiles,

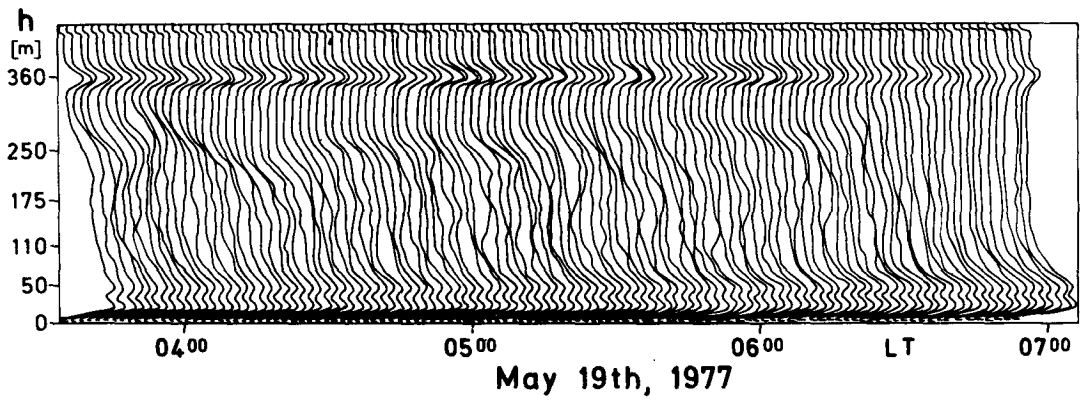

FIG. 13. Profiles of the relative backscatter amplitude.

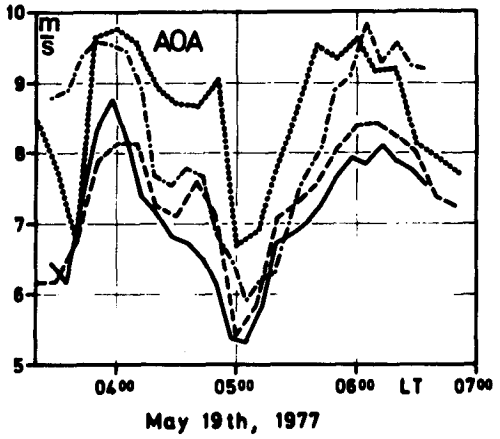

FIG. 14. Comparison between AOA and directly measured wind. AOA: solid line (0–84 m); direct: dashed line (50 m); AOA: dashed-dotted line (84–184 m); direct: dotted line (110 m).

however, also reveals a good behavior of the intermediate levels for heights $\gtrsim 30$ m.

Only AOA results obtained under stable conditions have been shown since no satisfactory wind measurements could be obtained during convective conditions. It is not presently clear whether this failure is one of principle or if it is surmountable by technical and data processing improvements.

Acknowledgments. Mr. B. Fischer did most of the programming and the help of Mr. H. Sievert in preparing and assisting with the experiments is gratefully acknowledged. We thank Prof. G. Stilke, who initiated the sodar activities at the Meteorological Institute in Hamburg, and his co-workers for support. We especially thank Mr. K. H. Praetorius and his staff of the Norddeutscher Rundfunk for permission to undertake this research at the tower site. The meteorological instrumentation at the antenna mast was supplied by the Deutsche Forschungsgemeinschaft.

This work was supported by the Bundes Ministerium der Verteidigung, the Sonderforschungsbereich 94 and the Deutsche Forschungsgemeinschaft.

REFERENCES

Aubry, M., 1975: Les sondages acoustiques de l'atmosphere. Exposé de synthése présenté à la XVIIIè Assemblée Générale de l'URSI, Lima, Note Technique CRPE/7, Centre National d'Études des Telecommunications, 23 pp.

Balser, M., C. A. McNary and A. E. Nagy, 1976: Remote wind sensing by acoustic radar. *J. Appl. Meteor.*, **15**, 50–58.

Beran, D. W., and B. C. Willmarth, 1971: Doppler winds from a bistatic acoustic sounder. *Preprints VII Int. Symp. Remote Sensing of Environment*, Ann Arbor, Willow Run Labs., The Univ. of Michigan, 1699–1714.

——, and S. F. Clifford, 1972: Acoustic Doppler measurements of the total wind vector. *Preprints Second Symp. Meteorological Observations and Instrumentation*, San Diego, Amer. Meteor. Soc.

——, C. G. Little and B. C. Willmarth, 1971: Acoustic Doppler measurements of vertical velocities in the atmosphere. *Nature*, **230**, 160–162.

Brown, E. H., 1972: Acoustic-Doppler-radar scattering equation and general solution. *J. Acoust. Soc. Amer.*, **52**, 1391–1396.

——, and S. F. Clifford, 1973: Spectral broadening of an acoustic pulse propagating through turbulence. *J. Acoust. Soc. Amer.*, **54**, 36–39.

——, 1974: Turbulent spectral broadening of backscattered acoustic pulses. *J. Acoust. Soc. Amer.*, **56**, 1398–1406.

Ford, G. W., and W. C. Meecham, 1960: Scattering of sound by isotropic turbulence of large Reynolds number. *J. Acoust. Soc. Amer.*, **32**, 1668–1672.

Gaynor, J. E., 1977: Acoustic Doppler measurement of atmospheric boundary layer velocity structure functions and energy dissipation rates. *J. Appl. Meteor.*, **16**, 148–155.

Hall, F. F., Jr., J. G. Edinger and W. D. Neff, 1975: Convective plumes in the Planetary Boundary Layer, investigated with an acoustic echo sounder. *J. Appl. Meteor.*, **14**, 513–523.

Mahoney, A. R., L. G. McAllister and J. R. Pollard, 1973: The remote sensing of wind velocity in the lower troposphere using an acoustic sounder. *Bound.-Layer Meteor.*, **4**, 155–167.

McAllister, L. G., 1972: Acoustic radar sounding of the lower atmosphere. *Proc. Workshop on Mathematics of Profile Inversion*, Ames Research Center, L. Colin, Ed., NASA TMX-62, 150 pp. (see pp. 2.2–2.12).

Monin, A. S., 1962: Characteristics of the scattering of sound in a turbulent atmosphere. *Sov. Phys. Acoust.*, **7**, 370–373.

Ottersten, H., 1969: Radar backscattering from the turbulent clear atmosphere. *Radio Sci.*, **4**, 1251–1255.

Owens, E. G., 1974: Microcomputer-controlled acoustic echo sounder. NOAA Tech. Memo. ERL WPL-21, 76 pp.

Peters, G., 1978: On the development of an acoustic sounder for wind measurements by the angle of arrival. Ph.D. dissertation, University of Hamburg, 80 pp.

Spizzichino, A., 1974: Discussion of the operating conditions of a Doppler sodar. *J. Geophys. Res.*, **79**, 5585–5591.

Stilke, G., C. Wamser and G. Peters, 1976: Untersuchungen über den Abbau einer Bodeninversion mit direkten und indirekten Meßverfahren. *Meteor. Rdsch.*, **29**, 181–186.

Tatarskii, V. J., 1971: *The Effects of the Turbulent Atmosphere on Wave Propagation* [Jerusalem, Israel Program for Scientific Translations, 472 pp].

Thompson, R. J., 1974: Ray-acoustic intensity in a moving medium. I. *J. Acoust. Soc. Amer.*, **55**, 729–732.

——, 1974: Ray-acoustic intensity in a moving medium. II. A stratified medium. *J. Acoust. Soc. Amer.*, **55**, 733–737.

Wamser, C., and H. Müller, 1977: On the spectral scale of wind fluctuations within and above the surface layer. *Quart. J. Roy. Meteor. Soc.*, **103**, 721–730.